Chapter 5

Glucosylation of stevioside by Gtf180-ΔN-Q1140E improves its taste profile

Tim Devlamynck[1], Koen Quataert[1], Evelien M. te Poele[2], Gerrit J. Gerwig[3], Johannis P. Kamerling[3], Wim Soetaert[1], Lubbert Dijkhuizen[2]

[1]Ghent University, [2]University of Groningen, [3]University of Utrecht

Abstract

The adverse health effects of sucrose overconsumption, typical for diets in developed countries, necessitate the use of low-calorie sweeteners. Since their approval by the European Commission in 2011, steviol glycosides have increasingly been used as high-intensity sweetener in food products. The most prevalent steviol glycoside in the leaves of *Stevia rebaudiana* is stevioside. Due to its lingering bitterness and off-flavors, it has found limited applications in food products, as the better tasting rebaudioside A (RebA) is preferred. Enzymatic glucosylation of stevioside is a well-known strategy to reduce this bitterness. Up to date, many glucosylation reactions of stevioside or RebA suffer from low productivities. In this chapter, the optimized α-glucosylation of stevioside with glucansucrase Gtf180-ΔN-Q1140E, previously shown to efficiently glucosylate RebA as well, is reported. The structures of the novel steviol glycosides were elucidated by NMR spectroscopy, mass spectrometry, and methylation analysis, revealing that stevioside was mainly glucosylated at the C-19 glucosyl moiety. In contrast to RebA glucosylation, minor products were also glucosylated at the C-13 site. Sensory analysis of the glucosylated stevioside products by a trained panel revealed significant reductions in bitterness and off-flavors compared to stevioside, while the typical intensive sweetness of steviol glycosides was retained.

1. Introduction

Over the past decade, Western society has increasingly been confronted with lifestyle diseases such as type 2 diabetes, ischaemic heart attacks and various cardiovascular diseases. The cost for society in Europe is estimated to be 2% to 4% of the total healthcare cost[213]. The risk to suffer from lifestyle diseases increases significantly when the BMI is higher than 25 kg/m^2 [214,215]. A study from Calle et al.[216] even revealed that 14% to 20% of all cancer deaths may also be related to overweight or obesity. Important causes of overweight are a decrease of physical activity and inappropriate dietary patterns. Moreover, an excessive sugar intake appears to be directly associated with an increase in body weight[217]. A wider array of sweet food products with less or even no sugar content is consequently a necessity in order to reduce the prevalence of lifestyle diseases.

Consumers are more and more aware of the relationship between diet-related diseases and healthy foods but are nevertheless not so eager to decrease their intake of sweet food products[218]. In addition, the 'natural' character of the applied sweeteners is increasingly perceived by consumers to be equally important as their taste[219]. The implementation into the market of natural, high-intensity sweeteners is thus driven by a strong consumer demand. Up to this date, several candidates have been proposed to take up this role: sweet-tasting proteins such as monatin and thaumatin[220], and other plant extracts like glycyrrhizin from the root of *Glycyrrhiza glabra*[221], mogrosides from monk fruit (*Siraitia grosvenorii*)[222], and steviol glycosides (SG) from the leaves of *Stevia rebaudiana*[186]. Since the European Commission authorized the use of high purity SG (≥95%), such as rebaudioside A (RebA) and stevioside (Stev), in foods and beverages, stevia-based products have rapidly expanded across the European market. Recently, it was shown that SG, by means of their steviol group, potentiate Ca^{2+}-dependent activity of TRPM5, a cation channel protein essential for taste transduction of sweet, bitter, and umami in chemosensory cells[223]. As a result, the sweetness of SG is intensified, whereas their bitterness lingers on. Interestingly, TRPM5 also facilitates insulin release by the pancreas, preventing high blood glucose

concentrations and consequently the development of type 2 diabetes[224]. A study on mice revealed that TRPM5 potentiation by SG protected them against the development of high-fat diet-induced hyperglycaemia, prompting the authors to propose SG as cost-effective antidiabetic drugs[225].

Unfortunately, roughly half of the human population attributes an unpleasant lingering bitterness to RebA and Stev, as reflected by the considerable sequence variation in the genes encoding for the bitter receptors hTAS2R4 and hTAS2R14[46]. One strategy to solve this issue consists in the addition of masking agents such as several sugar alcohols[226]. In order to circumvent the use of masking agents, enzymatic glucosylation of RebA and Stev has been proposed as a means to (partially) remove their bitterness[8]. Several enzymes, typically UDP-glucosyltransferases (UGTases)[57-59] and cyclodextrin glucanotransferases (CGTases)[50-56], have already been applied for this purpose. However, UGTases require expensive nucleotide-activated sugars as donor substrate[13], whereas CGTases possess poor C-13/C-19 regiospecificity, producing mixtures of α-glucosylated SG[51].

Alternatively, glucansucrases (GS) can be applied for the glucosylation of SG. GS (EC 2.1.4.-) are enzymes found only in lactic acid bacteria, of which most members, including *Lactobacillus reuteri*, have the generally-recognized-as-safe (GRAS) status. They use the donor substrate sucrose to catalyze the synthesis of α-glucan polysaccharides, thereby introducing different ratios of glycosidic linkages, depending on the enzyme specificity[75]. It was demonstrated that suppressing this α-glucan synthesis by mutational engineering improved the glucosylation of non-natural acceptor substrates such as catechol[110]. In chapter 4, the glucosylation of RebA with the Q1140E mutant of glucansucrase enzyme Gtf180-ΔN from *Lactobacillus reuteri* 180 was reported[68-70]. RebA was only glucosylated at the C-19 glucosyl moiety, producing mainly mono-α-glucosylated product with an (α1→6)-linkage, but also α-glucosides with two or more glucosyl units attached. The glucosylation of Stev, the most abundant steviol glycoside, was not addressed. Here, we report a careful optimization of the enzymatic glucosylation of Stev by the same enzyme. The structures of the two main α-

glucosylated Stev products were characterized by NMR spectroscopy, mass spectrometry, and methylation analysis. Sensory analysis by a trained panel revealed a substantial decrease in bitterness and off-flavors of the glucosylated products compared to Stev and RebA.

2. Materials and methods

2.1. Stevioside

Stevioside (>85 % purity, HPLC) was obtained from TCI Europe.

2.2. Production and purification of recombinant Gtf180-ΔN-Q1140E

Recombinant, N-terminally truncated Gtf180-ΔN from *Lactobacillus reuteri* 180 and derived Q1140E mutant were produced and purified as described previously[70,80,99].

2.3. Gtf180-ΔN-Q1140E activity assays

One unit (U) of enzyme activity corresponds to the conversion of 1 µmole sucrose (used for hydrolysis and transglycosylation) in a solution containing 100 mM sucrose, 25 mM sodium acetate (pH 4.7) and 1 mM $CaCl_2$, at 37 °C.

Enzyme activity assays were performed at 37 °C with 100 mM sucrose in 25 mM sodium acetate (pH 4.7) and 1 mM $CaCl_2$. Samples of 150 µL were taken every min over a period of 8 min and immediately inactivated with 30 µL 1 M NaOH. The sucrose concentrations of the samples were subsequently quantified by means of HPLC analysis (see HPLC analysis), allowing the calculation of the enzyme activity as defined above.

2.4. HPLC analysis

Two HPLC analyses were performed. For the analysis of glucose, fructose and sucrose, an Agilent MetaCarb 67H column (300 x 6.5 mm) was used under isocratic conditions with 2.5 mM H_2SO_4 as the mobile phase. The flow rate and temperature were set at 0.8 mL/min and 35 °C, respectively. Detection was achieved with an RI detector. Calibration of the obtained peaks was accomplished using the corresponding standard curves.

For the analysis of the steviol glycosides, an Agilent ZORBAX Eclipse Plus C18 column (100 x 4.6 mm, 3.5 µm) was used with water (solvent A) and acetonitrile (solvent B) as the mobile phase. The flow rate and temperature were set at 1.0 mL/min and 40 °C, respectively. Following gradient elution was used: 5-95% solvent B (0-25 min), 95% solvent B (25-27 min), 95-5% solvent B (27-30 min) and again 95% of solvent A (30-35 min). Detection was achieved with an ELS detector (evaporation temperature: 90 °C, nebulization temperature: 70 °C, gas flow rate: 1.6 SLM). Calibration of the obtained peaks was accomplished using the corresponding standard curves.

2.5. Design of response surface methodology experiment

Response surface methodology[198] was applied to optimize the Gtf180-ΔN-Q1140E catalyzed glucosylation of stevioside (acceptor substrate) with sucrose as donor substrate, while minimizing the synthesis of α-glucan oligosaccharides. All experiments were performed in 25 mM sodium acetate (pH 4.7), supplemented with 1 mM $CaCl_2$, at 37 °C. The addition of 10 U/mL enzyme ensured a steady-state was reached within 3 h of incubation. A Box-Behnken design[199] was generated implementing stevioside concentration (mM), sucrose/stevioside ratio (D/A ratio) and agitation rate (rpm) as factors. For each of them low (-1) and high (+1) level values were assigned as follows: stevioside concentration (25 mM) and (100 mM), D/A ratio (1) and (20), agitation rate (0 rpm) and (200 rpm). The experimental design was generated and analyzed using JMP software (release 12)[200] and consisted of 15 experiments carried out at 5

mL scale (Table SI). The response surface analysis module of JMP software was applied to fit the following second order polynomial equation:

$$\hat{Y} = \beta_0 + \sum_{i=1}^{I} \beta_i X_i + \sum_{i=1}^{I} \beta_{ii} X_i^2 + \sum_i \sum_j \beta_{ij} X_i X_j$$

where $\hat{Y}$ is the predicted response, I is the number of factors (3 in this study), β_0 is the model constant, β_i is the linear coefficient associated to factor X_i, β_{ii} is the quadratic coefficient associated to factor X_i^2 and β_{ij} is the interaction coefficient between factors X_i and X_j. X_i represents the factor variable in coded form:

$$X_{c,i} = \frac{[X_i - (low + high)/2]}{(high - low)/2}$$

with $1 \leq i \leq I$, where $X_{c,i}$ is the coded variable.

2.6. Production and purification of α-glucosylated stevioside

The production of α-glucosylated stevioside was performed at 50 mL scale in a shake flask, by incubating 31 mM stevioside and 524 mM sucrose with 10 U/mL Gtf180-ΔN-Q1140E at 37 °C in 25 mM sodium acetate (pH 4.7) and 1 mM $CaCl_2$ for 3 h. The α-glucosylated stevioside products were purified from the incubation mixture by flash chromatography using a Reveleris X2 flash chromatography system with a Reveleris C18 cartridge (12 g, 40 µm) with water (solvent A) and acetonitrile (solvent B) as the mobile phase (30 mL/min). Following gradient elution was used: 95% solvent A (0-2 min), 95-50% solvent A (2-20 min), 50-95% solvent B (20-22 min), 95% solvent B (22-25 min). Detection was achieved with UV (210 nm). The collected fractions were evaporated *in vacuo* and subsequently freeze dried to remove the residual water.

2.7. Alkaline hydrolysis of α-glucosylated stevioside and TLC analysis

To release the carbohydrate moiety linked to the C-19 carboxyl group, a 1 h stevioside incubation with Gtf180-ΔN-Q1140E (50 mM stevioside, 100 mM sucrose in 25 mM sodium acetate (pH 4.7) and 1 mM $CaCl_2$, 37 °C) was subjected to alkaline hydrolysis. Briefly, the stevioside incubation mixture was transferred into 1.0 M NaOH and heated at 80 °C for 2.5 h, then cooled down, and neutralized with 6 M HCl. Samples were spotted in lines of 1 cm on a TLC sheet (Merck Kieselgel 60 F254, 20x20 cm), which was developed in *n*-butanol:acetic acid:water = 2:1:1. Bands were visualized by orcinol/sulfuric acid staining and compared with a simultaneous run of standard compounds.

2.8. Methylation analysis

Steviol glycoside samples were permethylated using CH_3I and solid NaOH in $(CH_3)_2SO$, as described previously[227], then hydrolyzed with 2 M trifluoroacetic acid (2 h, 120 °C) to give a mixture of partially methylated monosaccharides. After evaporation to dryness, the mixture was dissolved in H_2O and reduced with $NaBD_4$ (2 h, room temperature). Subsequently, the solution was neutralized with 4 M acetic acid and boric acid was removed by repeated co-evaporation with methanol. The obtained partially methylated alditol samples were acetylated with 1:1 acetic anhydride-pyridine (30 min, 120 °C). After evaporation to dryness, the mixtures of partially methylated alditol acetates (PMAAs) were dissolved in dichloromethane and analyzed by GLC-EI-MS on an EC-1 column (30 m x 0.25 mm; Alltech), using a GCMS-QP2010 Plus instrument (Shimadzu Kratos Inc., Manchester, UK) and a temperature gradient (140-250 °C at 8 °C/min)[228].

2.9. Mass spectrometry

Matrix-assisted laser desorption ionization time-of-flight mass spectrometry (MALDI-TOF-MS) was performed on an AximaTM mass spectrometer (Shimadzu Kratos Inc.), equipped with a nitrogen laser (337 nm, 3 ns pulse width). Positive-ion mode spectra were recorded using the reflector mode at a resolution of 5000

FWHM and delayed extraction (450 ns). Accelerating voltage was 19 kV with a grid voltage of 75.2%. The mirror voltage ratio was 1.12 and the acquisition mass range was 200-6000 Da. Samples were prepared by mixing on the target 1 µL sample solutions with 1 µL aqueous 10% 2,5-dihydroxybenzoic acid in 70% acetonitrile as matrix solution.

2.10. NMR spectroscopic analysis

Resolution-enhanced 1D/2D 500-MHz $^{1}H/^{13}C$ NMR spectra were recorded in D_2O on a Bruker DRX-500 spectrometer (Bijvoet Center, Department of NMR Spectroscopy, Utrecht University). To avoid overlap of anomeric signals with the HOD signal, the 1D and 2D spectra were run at 310 K. Data acquisition was done with Bruker Topspin 2.1. Before analysis, samples were exchanged twice in D_2O (99.9 atom% D, Cambridge Isotope Laboratories, Inc., Andover, MA) with intermediate lyophilisation, and then dissolved in 0.6 mL D_2O. Fresh solutions of ~4 mg/mL were used for all NMR measurements. Suppression of the HOD signal was achieved by applying a WEFT (water eliminated Fourier transform) pulse sequence for 1D NMR experiments and by a pre-saturation of 1 s during the relaxation delay in 2D experiments. The 2D TOCSY spectra were recorded using an MLEV-17 (composite pulse devised by Levitt et al.[229]) mixing sequence with spin-lock times of 20, 50, 100 and 200 ms. The 2D ^{1}H-^{1}H ROESY spectra were recorded using standard Bruker XWINNMR software with a mixing time of 200 ms. The carrier frequency was set at the downfield edge of the spectrum in order to minimize TOCSY transfer during spin-locking. Natural abundance 2D ^{13}C-^{1}H HSQC experiments (^{1}H frequency 500.0821 MHz, ^{13}C frequency 125.7552 MHz) were recorded without decoupling during acquisition of the ^{1}H FID. The NMR data were processed using the MestReNova 9 program (Mestrelab Research SL, Santiago de Compostella, Spain). Chemical shifts (δ) are expressed in ppm by reference to internal acetone (δ_H 2.225 for ^{1}H and δ_C 31.07 for ^{13}C).

2.10 Sensory analysis

Sensory analysis was performed in individual tasting booths at the UGent Sensolab (Belgium) by a trained panel (7 persons), as described previously in chapter 4[70]. In short, taste (sweetness, liquorice, astringency and bitterness) was evaluated by swirling the sample in the mouth for 5 sec after which the sample was expectorated. Aftertaste was evaluated 10 sec after swallowing the solution. Lingering based on the maximum taste intensity was rated 1 min later. Sucrose reference solutions (5%, 7.5% and 10% sucrose, scoring 5, 7.5 and 10, respectively) were provided. Water (Spa Reine) and plain crackers were used as palate cleansers between sampling. All samples were evaluated in duplicate.

Statistical analyses were performed with SPSS 23 (SPSS Inc., Chicago, USA). All tests were done at a significance level of 0.05. One-Way ANOVA was used to investigate any significant difference between the solutions. Testing for equal variances was executed with the Modified Levene Test. When conditions for equal variance were fulfilled, the Tukey test[210] was used to determine differences between samples. In case variances were not equal, Games-Howell was performed[211].

Three different solutions sweetened with Stev products were examined: 588 mg/L mono-α-glucosylated product (Stev-G1), 588 mg/L multi-α-glucosylated product, containing residual Stev, Stev-G1 and higher α-glucosides (Stev-G) and 1176 mg/L multi-α-glucosylated product (Stev-G').

3. Results

3.1. Synthesis of α-glucosylated stevioside with Gtf180-ΔN-Q1140E

Gtf180-ΔN and the derived Gtf180-ΔN-Q1140E mutant also readily glucosylated stevioside. Optimization of the reaction conditions for rebaudioside A (RebA) glucosylation with Gtf180-ΔN-Q1140E revealed the importance of selecting

adequate concentrations of donor substrate sucrose and acceptor substrate RebA. The addition of too much sucrose resulted in suboptimal yields due to increased α-glucan synthesis[70]. The glucosylation of stevioside (Stev) was therefore also optimized by response surface methodology (RSM), using a Box-Behnken experimental design. Following factors were considered: X_1 Stev concentration (mM); X_2 the ratio of donor substrate sucrose over acceptor substrate Stev (D/A ratio); X_3 agitation speed (rpm). The addition of 10 U/mL enzyme ensured that a steady state in Stev conversion was obtained within 3 h. The results of the Box-Behnken experimental design are summarized in Table SI. The analysis of variance (ANOVA) showed R^2 values of 98.75% and 98.72% for Stev conversion degree (%) and amount of α-glucosylated Stev (Stev-G) synthesized (mM), respectively. The effects of the factors were analyzed applying the response surface contour plots (Figure 1).

Higher Stev conversion degrees were obtained at decreasing Stev concentrations, independent on the concentration of donor substrate sucrose. The effect of the D/A ratio on Stev conversion degrees displayed a distinct optimum, similarly to RebA glucosylation with Gtf180-ΔN-Q1140E[70]. An increase of D/A ratio initially resulted in improved Stev conversion degrees, indicating that sucrose drives the reaction. However, as sucrose also acts as primer for α-glucan synthesis, a further increase of D/A ratio resulted in less Stev glucosylation in favor of more α-glucan synthesis. This confirmed that the concentrations of sucrose and Stev need to be carefully optimized. In contrast, the effect of agitation on Stev conversion degrees and amount of Stev-G synthesized was negligible.

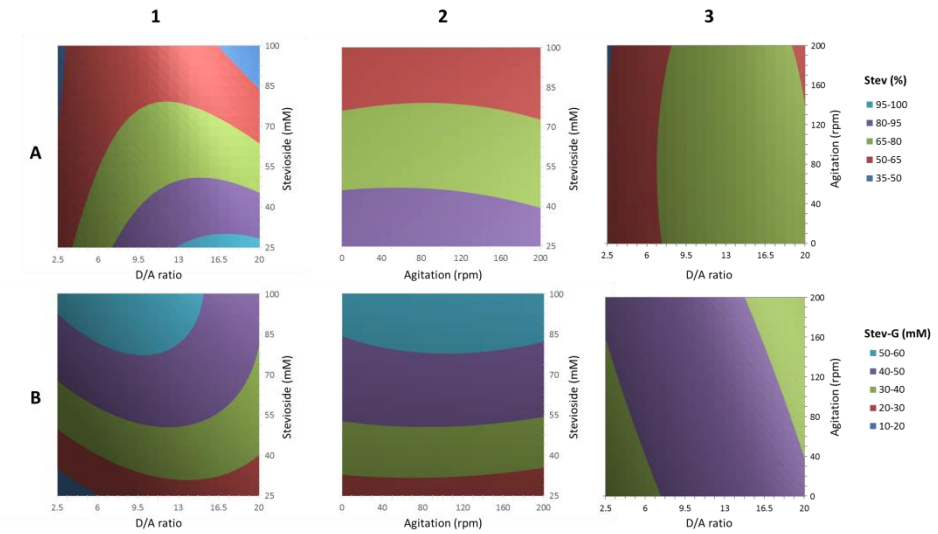

Figure 1. Response surface methodology contour plots of stevioside glucosylation by Gtf180-ΔN-Q1140E, showing the effects of: Stev concentration (mM); D/A ratio (ratio of donor substrate sucrose over acceptor substrate Stev); agitation (rpm) on: (**A**) Stev conversion degree (%); (**B**) Stev-G synthesized (mM).

The resulting model was consequently used for the optimization of the reaction conditions. An efficient conversion of Stev into Stev-G (at least 95%), yielding a maximal amount of Stev-G, was targeted. The model predicted the synthesis of 29 mM Stev-G in case following conditions were applied: 31 mM Stev, 524 mM sucrose (D/A ratio of 16.9) and 0 rpm. The validation test resulted in the synthesis of 28 mM Stev-G (Figure 2A), which was in good agreement with the prediction. Compared to RebA glucosylation with Gtf180-ΔN-Q1140E[70], much more donor substrate sucrose was needed to completely convert Stev (D/A ratio of 16.9 compared to 3.4), whereas less glycosylated product could be obtained (28 mM compared to 80 mM), indicating that the enzyme has a lower affinity for Stev than for RebA. Equally remarkable was that while RebA was mainly converted into mono-α-glucosylated product (RebA-G1, 77.7%), Stev was only for 32.5% converted into mono-α-glucosylated product (Stev-G1). Applying the optimal conditions for the glucosylation of Stev with wild type Gtf180-ΔN resulted only in the conversion of 60.9% Stev with a Stev-G1/Stev-G ratio of 23.7% (Figure 2B).

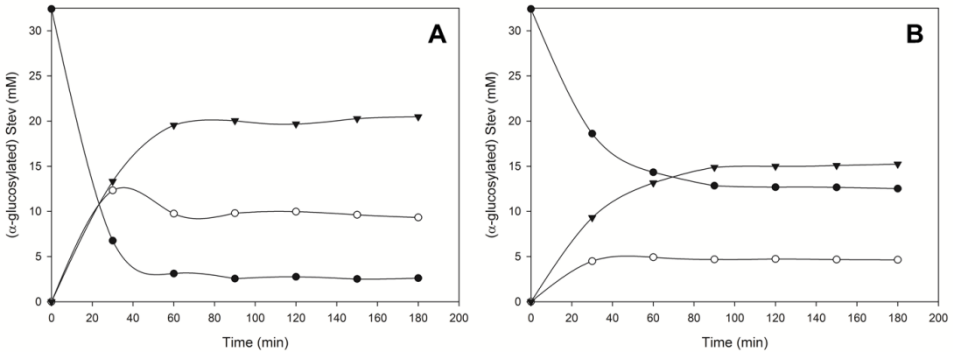

Figure 2. Time course of stevioside glucosylation by Gtf180-ΔN-Q1140E (**A**) and Gtf180-ΔN (**B**) at optimal batch conditions (31 mM Stev; 524 mM sucrose; 10 U/mL enzyme). ● Stev ○ Stev-G1 ▼ Stev-G2+.

3.2. Structural characterization of α-glucosylated stevioside products

Incubation of 31 mM Stev and 524 mM sucrose with Gtf180-ΔN-Q1140E resulted in the synthesis of several α-glucosylated stevioside products (Figure 3). The 2 main products (Stev-G1 and Stev-G2) were analyzed by a combination of 1D and 2D NMR spectroscopy, methylation analysis and mass spectrometry. Detailed structural analysis of novel steviol glycosides is of great value, since the sensory properties are known to depend on the number, location and configuration of the introduced glycosyl moieties[8]. Figure 4 depicts the 1D ^{1}H NMR spectra while Figure 5 shows the corresponding chemical structures. The ^{1}H and ^{13}C chemical shifts are presented in Tables SII and SIII.

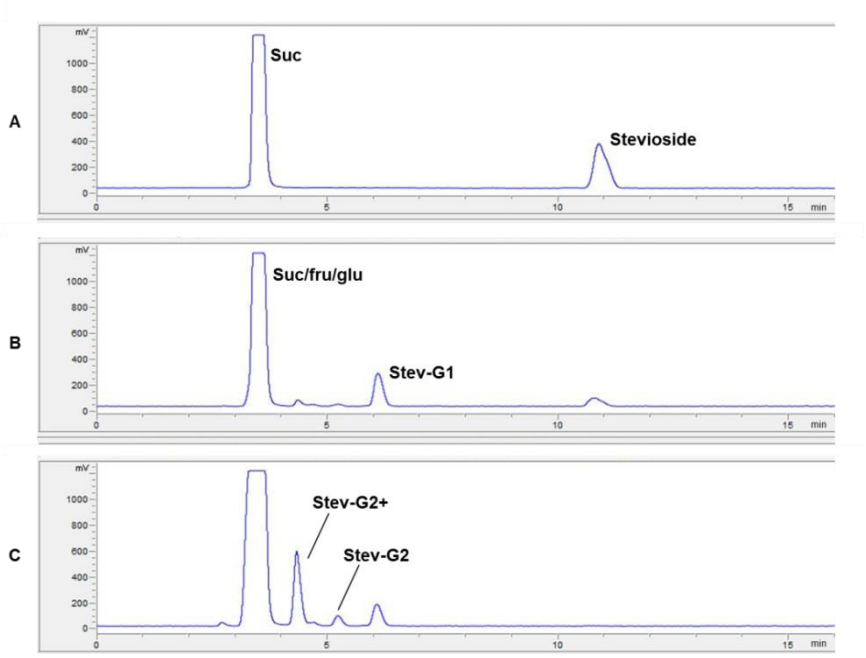

Figure 3. HPLC separation profiles of a 3 h incubation of 31 mM Stev and 524 mM sucrose with 10 U/mL Gtf180-ΔN-Q1140E. **A** 0 min, **B** 30 min, **C** 180 min of incubation at 37 °C. **Suc** sucrose, **fru** fructose, **glu** glucose.

3.2.1. Stev-G1

Methylation analysis (Table SIV) of Stev-G1 (Stev+1Glc, according to MALDI-TOF-MS: *m/z* 989.7 $[M+Na]^+$ (Figure 6B)) showed terminal Glc*p*, 2-substituted Glc*p* and 6-substituted Glc*p* (molar ratio 2:1:1), indicating that transglucosylation had resulted in elongation but not in branching. The ^{1}H NMR spectrum of Stev-G1 (Figure 4B) showed resonances of one main α-glucosylated Stev product, however, with five small (anomeric) signals (indicated with *: δ_H 5.35, 4.45, 4.14, 3.98, 3.16 in Figure 4B) of extra compounds (<10%). The spectrum between 0.8 and 2.2 ppm represented the typical steviol core signal pattern as seen for Stev (Figure 4A). Besides the three β-anomeric ^{1}H signals related to Stev (Glc1, δ_H 5.415; Glc2, δ_H 4.725; Glc3, δ_H 4.675), one extra anomeric ^{1}H resonance (δ_H 4.862; $J_{1,2}$ 3.7 Hz), partially overlapping with one steviol C-17 proton, was

observed, stemming from a new α-linked Glc residue (Glc4). The latter ^{1}H signal correlated with a ^{13}C resonance at δ_C 99.3 in the HSQC spectrum (Figure S1).

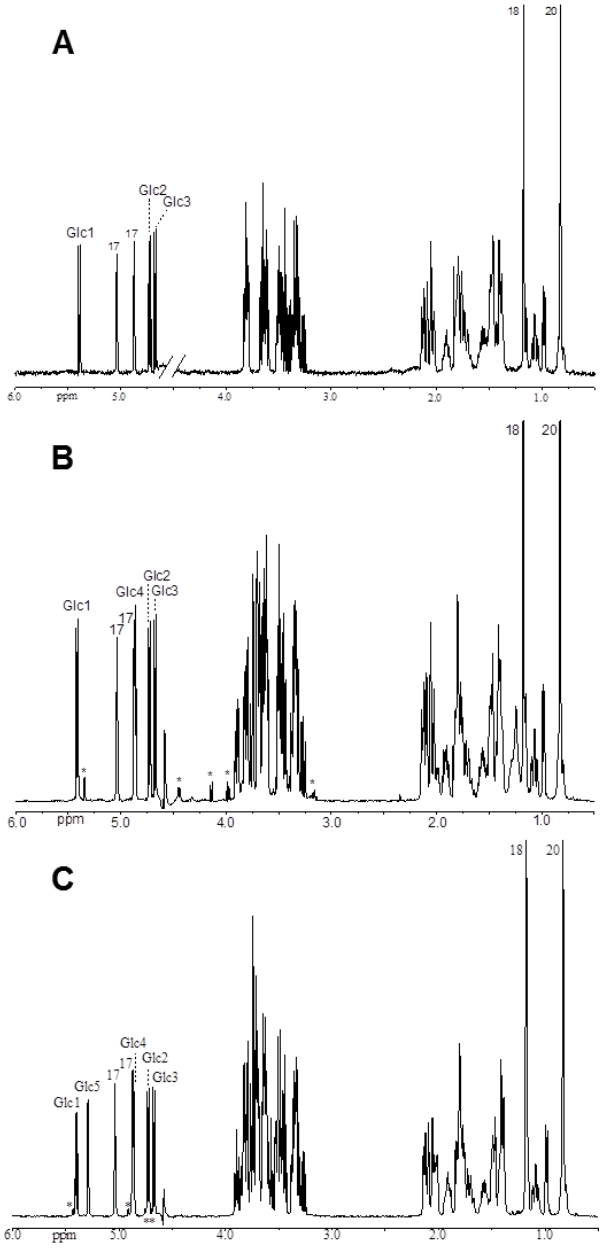

Figure 4. 500-MHz ^{1}H NMR spectrum of Stev (**A**), Stev-G1 (**B**), and Stev-G2 (**C**), recorded in D_2O at 310 K. * Resonances stemming from additional product(s).

Applying 2D NMR spectroscopy (TOCSY with different mixing times, ROESY and HSQC), the $^{1}H/^{13}C$ chemical shifts of the steviol core (Table SII) and the four Glc residues (Table SIII) of Stev-G1 were assigned (Figure S1). The ^{1}H and ^{13}C chemical shift sets of Glc2 and Glc3 correspond to those of Stev, suggesting that no modifications had occurred in the carbohydrate moiety at the steviol C-13 site. The TOCSY Glc4 H-1 track (δ_H 4.862) showed the complete scalar coupling network H-1,2,3,4,5,6a,6b, and combined with the Glc4 C-1–C-6 set of chemical shifts (HSQC), a terminal Glc(α1→6) unit is indicated. Based on the inter-residual ROESY cross-peaks between Glc4 H-1 (δ_H 4.862) and Glc1 H-6a/b (δ_H 3.89/3.70), combined with the ^{13}C downfield shift of 4.5 ppm for Glc1 C-6 (δ_C 66.7; Stev Glc1 C-6: δ_C 62.2) (HSQC spectrum, Figure S1), a Glc4(α1→6)Glc1 disaccharide element could be established[69].

The conclusive structure of the main compound in Stev-G1 was consequently determined as Stev elongated with a Glc*p*(α1→6) residue at the Glc1(β1→ on the C-19 site of the steviol core (Figure 5B).

3.2.2. Stev-G2

Methylation analysis (Table SIV) of Stev-G2 (Stev+2Glc, according to MALDI-TOF-MS: *m/z* 1152.0 $[M+Na]^+$ (Figure 6C)) showed terminal Glc*p* and 2-substituted Glc*p*, 4-substituted Glc*p*, and 6-substituted Glc*p* (molar ratio 2:1:1:1), together with a trace amount (<2%) of 2,6-substituted Glc*p*. The ^{1}H NMR spectrum of Stev-G2 (Figure 4C) exhibited the typical steviol core signal pattern as seen for Stev (Figure 4A). Besides the three β-anomeric ^{1}H carbohydrate signals related to Stev (Glc1, δ_H 5.415; Glc2, δ_H 4.727; Glc3, δ_H 4.674), two α-anomeric ^{1}H resonances of equal intensity (δ_H 4.863; $J_{1,2}$ 3.9 Hz and δ_H 5.292; $J1_{,2}$ 3.7 Hz) were observed, stemming from two new α-linked Glc residues (Glc4 and Glc5). The ^{1}H NMR spectrum indicated the presence of one main di-α-glucosylated Stev product, together with very minor products (<10%) represented by four small anomeric signals (indicated with *: δ_H 5.43, 4.91, 4.75, 4.71 in Figure 4C).

Using 2D NMR spectroscopy (TOCSY with different mixing times, ROESY and HSQC), the $^{1}H/^{13}C$ chemical shifts of the steviol core (Table SII) and the five Glc residues (Table SIII) of Stev-G2 (main compound) were assigned (Figure S2)[69]. The ^{1}H and ^{13}C chemical shift sets of Glc2 and Glc3 correspond closely with those of Stev and Stev-G1, suggesting that no modifications had occurred in the carbohydrate moiety at the steviol C-13 site.

However, the TOCSY Glc4 H-1 track (δ_H 4.863) showed a scalar coupling network H-1,2,3,4,5,6a,6b, different from that of Glc4 in Stev-G1, in particular H-3 (δ_H 3.90) and H-4 (δ_H 3.58), and together with the ^{13}C chemical shift of Glc4 C-4 (δ_C 77.9, 4, $\Delta\delta_C$ 6.6 ppm), a 4-substituted Glc4 residue is indicated (in accordance with the methylation analysis). The HSQC spectrum (Figure S2) showed a Glc1 C-6 (16a-16b) downfield shift ($\Delta\delta_C$ 5.2 ppm) as earlier observed for Glc1 in Stev-G1 ($\Delta\delta_C$ 4.5 ppm), indicating the presence of the Glc4(α1→6)Glc1 disaccharide element, leading to the establishment of a Glc5(α1→4)Glc4(α1→6)Glc1 trisaccharide linked to the C-19 of the steviol core. The inter-residual ROESY cross-peaks (spectrum not shown) between Glc4 H-1 (δ_H 4.863) and Glc1 H-6a/b (δ_H 3.85/3.74) and between Glc5 H-1 (δ_H 5.292) and Glc4 H-4 (δ_H 3.58) confirmed the glycosidic linkages between the three Glc residues. Furthermore, the 4-substitution of Glc4 was supported by the typical $^{1}H/^{13}C$ chemical shifts of its H-3/C-3 (43, δ_H 3.90 / δ_C 74.8) in the HSQC spectrum (Figure S2).

The conclusive structure of the main compound in Stev-G2 is consequently Stev elongated with a Glc*p*(α1→4)Glc*p*(α1→6) element at the Glc1(β1→ residue on the C-19 site of the steviol core (Figure 5C).

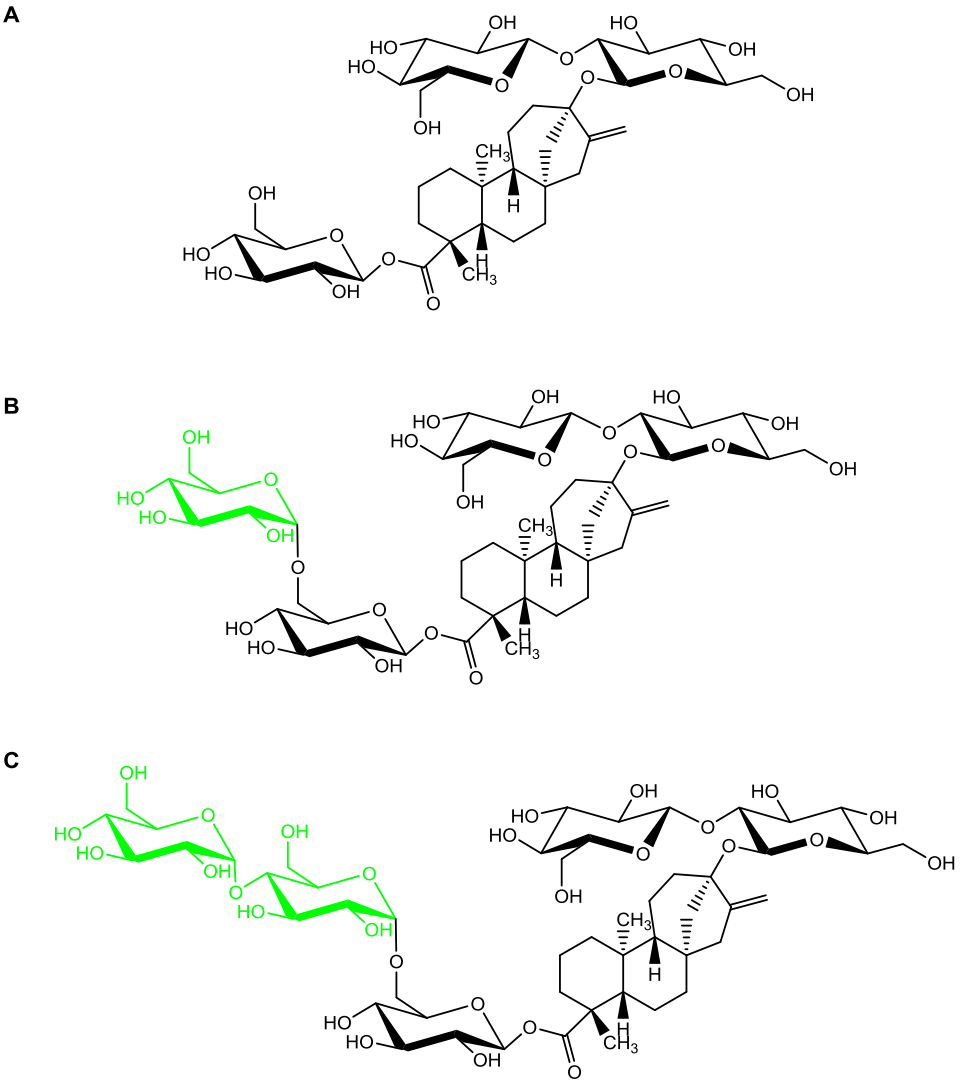

Figure 5. Chemical structures of Stev (**A**), Stev-G1 (**B**), and Stev-G2 (**C**).

3.2.3 Stev-G

Besides Stev-G1 and Stev-G2, Stev-G was composed of a wide array of α-glucosylated Stev products (Stev-G2+), as demonstrated by MALDI-TOF mass spectrometry, showing the *m/z* $[M+Na]^+$ peaks of Stev+1Glc up to Stev+9Glc (Figure 6D). It has to be noted that each peak may contain more than one compound, as different glycosidic linkage types may be present. Indeed,

methylation analysis (data not shown) showed six partially methylated alditol acetates, indicating the complexity of the Stev-G2+ mixture.

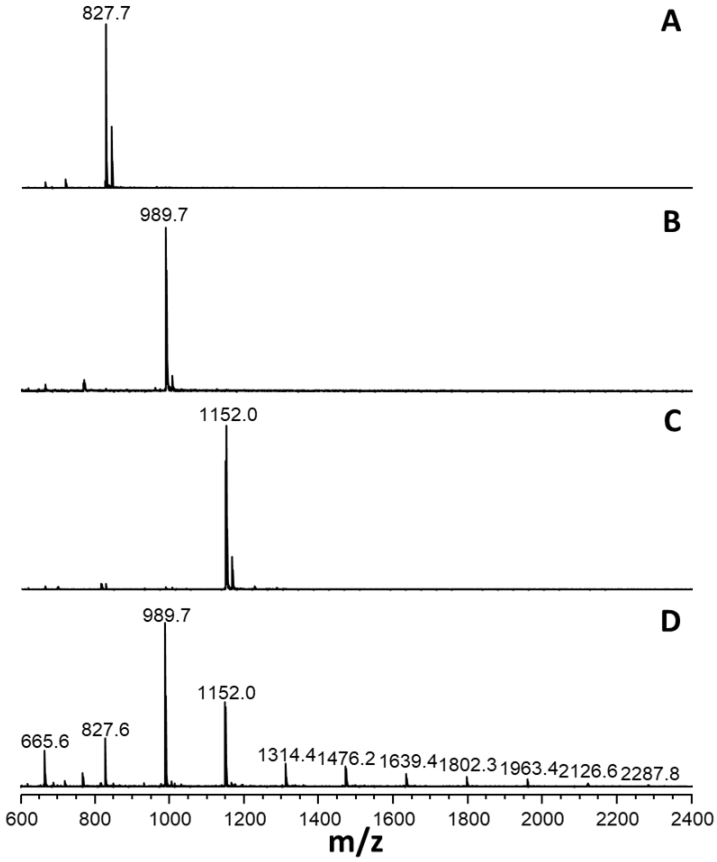

Figure 6. MALDI-TOF mass spectra of (**A**) Stev, (**B**) Stev+1Glc, (**C**) Stev+2Glc, (**D**) Stev-G. The α-glycosylated Stev products were obtained after incubation with Gtf180-ΔN-Q1140E and removal of residual carbohydrates. Mass peaks could be assigned to *m/z* $[M+Na]^+$ values of Stev+1Glc (989.7), Stev+2Glc (1152.0), up to Stev+9Glc (2287.8).

Alkaline hydrolysis of the Stev-G mixture suggested that Stev was not specifically glucosylated at the C-19 site but also at the C-13 site (Figure 7). Indeed, treatment of Stev with NaOH resulted in hydrolysis of the C-19-ester group, yielding steviolbioside. Therefore, the appearance of a product spot representing the same size as Stev after alkaline hydrolysis of Gtf180-ΔN-Q1140E-glycosylated Stev might suggest the formation of steviolbioside with one extra

glucose at the C-13 site. In other words, Stev-G2+ contains products glucosylated at the C-13 site, in contrast to RebA-G2+ which is completely composed of RebA products glucosylated at the C-19 site. Further structural analysis by means of NMR spectroscopy is nevertheless needed to confirm these results.

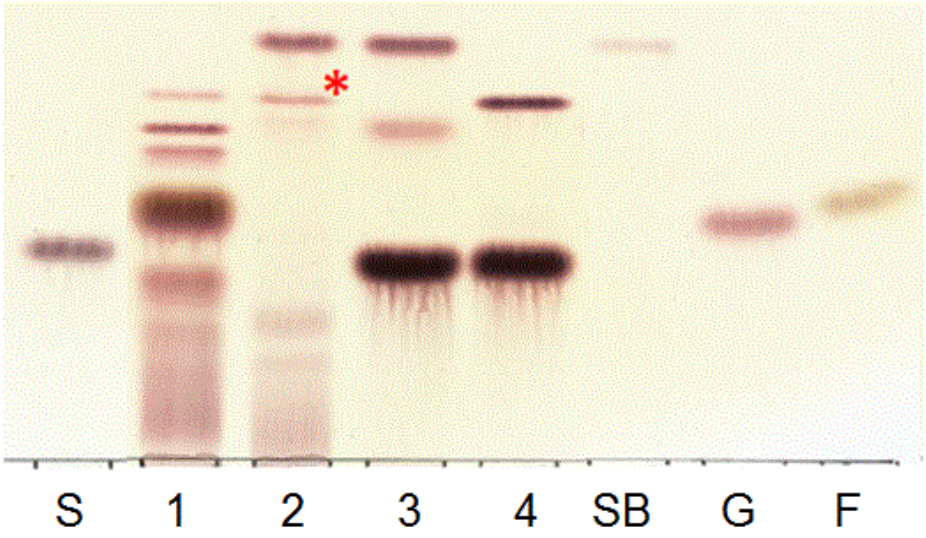

Figure 7. Alkaline hydrolysis of α-glucosylated stevioside (Stev-G) produced by Gtf180-ΔN-Q1140E. **S** sucrose, **1** Stev incubation (1 h), **2** Stev incubation (1 h) + NaOH, **3** Stev incubation (0 h) + NaOH, **4** Stev incubation (0 h), **SB** steviolbioside, **G** glucose, **F** fructose. * might suggest the formation of a product with the same size as stevioside, i.e. steviolbioside with one extra glucose at the C-13 site.

3.3. Sensory analysis of glucosylated stevioside products

The (α1→6)-glucosylation of Stev at the C-19 site is reported to improve its taste quality, mostly by alleviating its bitterness and off-flavors[66]. A sensory analysis of aqueous solutions sweetened with Stev and several glucosylated Stev products was performed by a trained panel, evaluating 9 different taste attributes. Three different product solutions were examined: 588 mg/L mono-α-glucosylated product (Stev-G1), 588 mg/L multi-α-glucosylated product, containing residual

Stev, Stev-G1 and higher α-glucosides (Stev-G) and 1176 mg/L multi-α-glucosylated product (Stev-G'). The mean scores of the taste attributes of the sweetened solutions are shown in Figure 8.

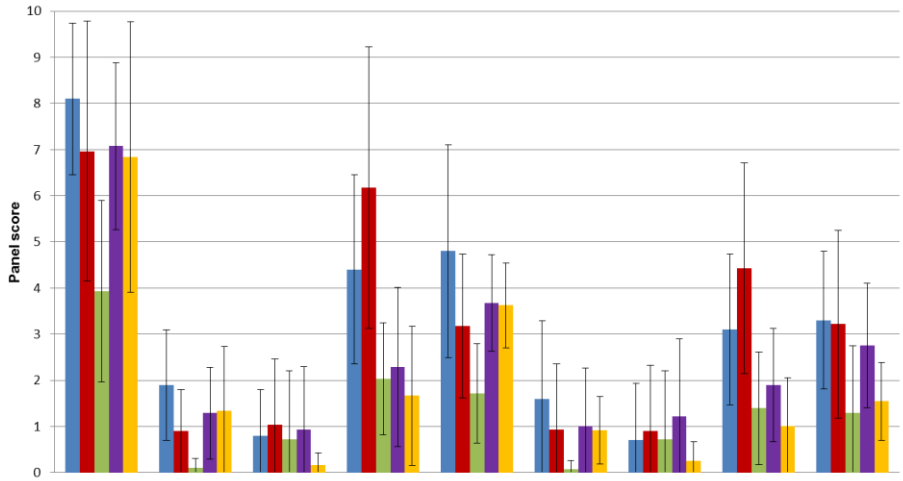

Sample	Taste				Aftertaste				Lingering
	Sweet	Liquorice	Astringent	Bitter	Sweet	Liquorice	Astringent	Bitter	
RebA	8.1^{A}	1.9^{A}	0.8^{A}	4.4^{AB}	4.8^{A}	1.6^{A}	0.7^{A}	3.1^{AB}	3.3^{A}
Stev	7.0^{A}	0.9^{A}	1.0^{A}	6.2^{A}	3.2^{A}	0.9^{AB}	0.9^{A}	4.0^{A}	3.2^{A}
Stev-G	3.9^{B}	0.1^{B}	0.7^{A}	2.0^{B}	1.7^{B}	0.1^{B}	0.7^{A}	1.4^{B}	1.3^{B}
Stev-G1	7.1^{A}	1.3^{A}	0.9^{A}	2.3^{B}	3.7^{A}	1.0^{AB}	1.2^{A}	1.9^{B}	2.8^{A}
Stev-G'	6.8^{A}	1.3^{AB}	0.2^{A}	1.7^{B}	3.6^{A}	0.9^{AB}	0.3^{A}	1.0^{B}	1.5^{B}

Figure 8. Sensory analysis of stevioside (Stev), Stev-G, Stev-G1 and Stev-G'. ^{A,B}: different letters indicate significant differences ($p<0.05$) between solutions following one-way ANOVA and post-hoc test.

All α-glucosylated stevioside products were significantly less bitter than stevioside. Stev-G1 retained the very high sweetness typical for steviol glycosides such as stevioside. In contrast, Stev-G was significantly less sweet than stevioside, which can be explained by the relatively large proportion of multi-α-glucosylated products. Multi-α-glucosylation resulted not only in a further decrease of bitterness, but simultaneously decreased sweetness as well. In addition, Stev-G was also significantly less liquorice and lingering than stevioside (Figure 8). Doubling the concentration of Stev-G from 588 mg/L to 1176 mg/L

roughly resulted in a duplication of the sweetness, equaling the sweetness level of stevioside, whereas bitterness and off-flavors were still equally suppressed. Glucosylation of stevioside with Gtf180-ΔN-Q1140E is thus a very adequate method to improve its sensory properties, i.e. by reducing the typical bitterness to a very low level.

4. Discussion

Even though Stev is the most abundant of all steviol glycosides extracted from the leaves of the *Stevia* plant, its lingering bitterness prevents applications in low-calorie foods and beverages. All current *Stevia* food products are based on RebA, perceived as less bitter than Stev, implying that the latter is discarded as a "side product". This chapter demonstrated that the α-glucosylation of Stev with Gtf180-ΔN-Q1140E offers a viable method to significantly reduce its bitterness. A very high Stev conversion of 95%, yielding 50 g/L Stev-G within 3 h, while using only 10 U/mL enzyme, was obtained after optimization of the reaction conditions by RSM. Structural analysis revealed that Stev was mostly glucosylated at the C-19 site, initially through an (α1→6)-linkage, after which the synthesized Stev-G1 was glucosylated through an (α1→4)-linkage, yielding Stev-G2 (Figure 5). MALDI-TOF and MS analysis indicated that a complex mixture of many other multi-glucosylated products (> 50% of Stev-G) was formed by the enzyme, as opposed to RebA α-glucosylation by Gtf180-ΔN-Q1140E, resulting in the synthesis of mostly mono-α-glycosylated product (77%)[70]. As a consequence, Stev-G was perceived half as sweet as Stev, an undesired effect which could be compensated by doubling the dose of Stev-G. Remarkably, this did not affect the significantly reduced perception of bitterness nor of other off-flavors.

A previous study already reported the application of a dextransucrase from *Leuconostoc citreum* KM20[66] for the glucosylation of Stev: a high conversion degree (94%) was obtained, however, much more enzyme (4500 U/mL vs. 10 U/mL) and a longer incubation time (5 days vs. 3 h) was needed. The volumetric productivity per U enzyme of the mutant Gtf180-ΔN-Q1140E enzyme reaction is

consequently more than 2,000 times higher. Transglucosylation of stevioside, using sucrose as donor substrate, was also achieved with an alternansucrase (EC 2.4.1.140) from *L. citreum* SK24.002, an enzyme that also makes (α1→6) and (α1→3) linkages[67,230,231]. Under optimized reaction conditions, a maximum conversion degree of only 44% was achieved. Stevioside was elongated at the terminal Glc(β1→2) residue of the β-sophorosyl unit at the steviol C-13 site with an (α1→6) linkage. Also a tri-glucosyl-stevioside was structurally characterized and was shown to be a (α1→3)-(α1→6)-(α1→3) extension at the terminal Glc(β1→2) residue at C-13. A taste comparison of the products was not reported. In addition, a mono-glucosylated stevioside product, containing a Glc(α1→6) residue at the steviol C-19-ester-linked Glc(β1→ residue (comparable with Stev-G1), has been synthesized with β-amylase Biozyme L and maltose as glucose donor. This also led to an improvement in quality of taste[60], just like shown here for the Gtf180-ΔN-Q1140E products. However, also products elongated at the C-13 site were synthesized, resulting in a decreased quality of taste.

These examples illustrate the three main requirements for any enzymatic Stev glucosylation process: an adequate product specificity, a complete Stev conversion and a high space-time yield. The here described process is clearly superior to the other glucansucrase-catalyzed Stev glucosylation reactions, adequately meeting all three requirements.

5. Supplementary information

Table SI. Box-Behnken experimental design and results for the variables studied. Second-degree polynomial equation with coefficients of each factor is given for amount of Stev-G synthesized (mM) and stevioside conversion degree (%). **X_1** stevioside (mM), **X_2** D/A ratio, **X_3** agitation (rpm).

	Pattern	X_1	X_2	X_3	Stev-G (mM) [1]	Stev conversion (%) [2]
1	+0+	100	11.25	200	55.5	55.5
2	0−+	62.5	2.5	200	28.3	45.3
3	−0+	25	11.25	200	22.5	90.0
4	0−−	62.5	2.5	0	30.3	48.5
5	++0	100	20	100	38.1	38.1
6	−0−	25	11.25	0	23.2	92.9
7	−+0	50	20	20	23.7	94.8
8	0+−	62.5	20	0	42.9	68.6
9	−−0	25	2.5	100	14.8	59.3
10	000	62.5	11.25	100	44.9	71.8
11	+−0	100	2.5	100	51.6	51.6
12	000	62.5	11.25	100	45.2	72.4
13	000	62.5	11.25	100	45.6	72.9
14	0++	62.5	20	200	39.8	63.6
15	+0−	100	11.25	0	53.2	53.2

[1] $\text{Stev-G} = 45.0500 + 14.2725X_1 - 0.1875X_2 - 0.1900X_3 - 5.6000X_1X_2 + 0.7550X_1X_3 - 5.5250X_2X_3 - 5.1100X_1^2 - 7.8900X_2^2 - 1.3350X_3^2$

[2] $\text{Stev conversion} = 72.1000 - 17.3225X_1 + 7.5500X_2 - 1.0975X_3 - 12.2500X_1X_2 + 1.2950X_1X_3 - 0.4500X_2X_3 - 2.6225X_1^2 - 13.7725X_2^2 - 1.8275X_3^2$

Table SII. ^{1}H and ^{13}C chemical shifts (δ)[a] for the steviol part of Stev, Stev-G1, and Stev-G2, recorded in D_2O at 310 K. For chemical structures, see Figure 5.

Carbon[b] number	Stev		Stev-G1		Stev-G2	
	δ ^{1}H	δ ^{13}C	δ ^{1}H	δ ^{13}C	δ ^{1}H	δ ^{13}C
1	0.82	41.4	0.82	41.3	0.83	41.3
	1.82		1.82		1.82	
2	1.31	20.3	1.30	20.3	1.30	20.3
	1.60		1.60		1.51	
3	1.07	38.5	1.07	38.5	1.09	38.6
	2.05		2.04		2.04	
5	1.16	57.7	1.16	57.7	1.17	57.7
6	1.66	22.1	1.68	22.8	1.82	22.9
	1.81		1.80		2.04	
7	1.40	42.0	1.43	42.1	1.42	42.1
	1.49		1.47		1.49	
9	0.98	54.4	0.98	54.2	0.98	54.4
11	1.68	22.7	1.70	22.9	1.66	22.9
	1.83		1.83		1.80	
12	1.48	37.5	1.48	37.6	1.48	37.5
	1.90		1.90		1.90	
14	1.39	45.6	1.40	45.5	1.41	45.5
	2.13		2.12		2.13	
15	2.06	48.2	2.06	48.1	2.05	48.1
	2.10		2.09		2.08	
17	4.87	105.4	4.87	105.4	4.87	105.4
	5.04		5.04		5.04	
18	1.18	29.2	1.18	29.3	1.18	29.2
20	0.83	16.4	0.83	16.5	0.83	16.4

[a] In ppm relative to internal acetone (δ 2.225 for ^{1}H and δ 31.07 for ^{13}C).

[b] As ^{13}C data have been deduced from HSQC measurements, ^{13}C chemical shifts in D_2O are missing for C-4, C-8, C-10, C-13, C-16 and C-19.

Table SIII. ^{1}H and ^{13}C chemical shifts (δ)[a] for the Glc*p* residues of Stev, Stev-G1, and Stev-G2, recorded in D_2O at 310 K. For chemical structures, see Figure 5.

Residue	Stev		Stev-G1		Stev-G2	
	δ ^{1}H	δ ^{13}C	δ ^{1}H	δ ^{13}C	δ ^{1}H	δ ^{13}C
Glc1(β1→C-19)						
H-1	5.40	95.4	5.41	95.5	5.41	95.4
H-2	3.46	73.6	3.46	73.0	3.45	73.4
H-3	3.50	78.0	3.50	77.8	3.50	77.9
H-4	3.40	70.7	3.45	70.6	3.45	70.6
H-5	3.50	77.7	3.70	77.0	3.70	76.9
H-6a	3.82	62.2	3.89	*66.7*	3.85	*67.4*
H-6b	3.67		3.70		3.74	
Glc2(β1→C-13)						
H-1	4.73	97.2	4.72	97.3	4.73	97.2
H-2	3.49	*82.2*	3.49	*82.2*	3.49	*82.1*
H-3	3.62	77.6	3.62	77.7	3.62	77.6
H-4	3.34	71.2	3.34	71.1	3.35	71.0
H-5	3.33	77.2	3.34	77.4	3.34	77.2
H-6a	3.80	62.2	3.80	62.2	3.80	62.2
H-6b	3.63		3.63		3.65	
Glc3(β1→2)						
H-1	4.67	104.3	4.67	104.5	4.67	104.4
H-2	3.26	75.7	3.27	75.8	3.27	75.8
H-3	3.45	77.0	3.45	77.3	3.45	77.0
H-4	3.32	71.2	3.34	71.1	3.33	71.2
H-5	3.35	77.4	3.34	77.4	3.35	77.2
H-6a	3.82	62.2	3.82	62.2	3.82	62.2
H-6b	3.64		3.64		3.64	
Glc4			(α1→6)**Glc1**		(α1→6)**Glc1**	
H-1			4.86	99.3	4.86	99.2
H-2			3.48	73.0	3.53	72.9
H-3			3.65	74.4	3.90	74.8
H-4			3.36	71.3	3.58	*77.9*
H-5			3.62	73.5	3.70	71.7
H-6a			3.75	62.0	3.75	61.8
H-6b			3.68		3.70	
Glc5					(α1→4)**Glc4**	
H-1					5.29	101.6
H-2					3.52	73.1

H-3	3.63	74.3
H-4	3.37	71.0
H-5	3.64	74.3
H-6a	3.78	61.8
H-6b	3.70	

[a] In ppm relative to the signal of internal acetone (δ 2.225 for ^{1}H and δ 31.07 for ^{13}C).

[b] Substituted carbon positions are indicated in *italics*.

Table SIV. Methylation analysis of the carbohydrate moieties in Stev, Stev-G1, and Stev-G2.

PMAA	R_t[a]	Structural feature	Peak area (%)[b]		
			Stev	Stev-G1	Stev-G2
2,3,4,6-Hex[c]	1.00	Glc*p*(1→	66	52	42
3,4,6-Hex	1.15	→2)Glc*p*(1→	34	25	21
2,3,6-Hex	1.18	→4)Glc*p*(1→	-	-	19
2,3,4-Hex	1.22	→6)Glc*p*(1→	-	23	18
3,4-Hex	1.39	→2,6)Glc*p*(1→	-	-	tr[d]

[a] R_t, retention time relative to 1,5-di-*O*-acetyl-2,3,4,6-tetra-*O*-methylglucitol (1.00) on GLC.

[b] Average values from triplo determination (not corrected by response factors).

[c] 2,3,4,6-Hex = 1,5-di-*O*-acetyl-2,3,4,6-tetra-*O*-methylhexitol-1-*d*, etc.

[d] tr = trace (<2%).

Figure S1. HSQC, TOCSY and ROESY spectrum of the carbohydrate part of Stev-G1, recorded in D_2O at 310 K. In HSQC, 22 means cross-peak H-2/C-2 of residue Glc2, etc. 16a-16b means cross-peaks H-6's/C-6 of residue Glc1, shifted downfield ($\Delta\delta_C$ 4.5 ppm) due to substitution Glc4(α1→6)Glc1. Significant cross-peaks, concerning glycosidic linkages, are indicated in red.

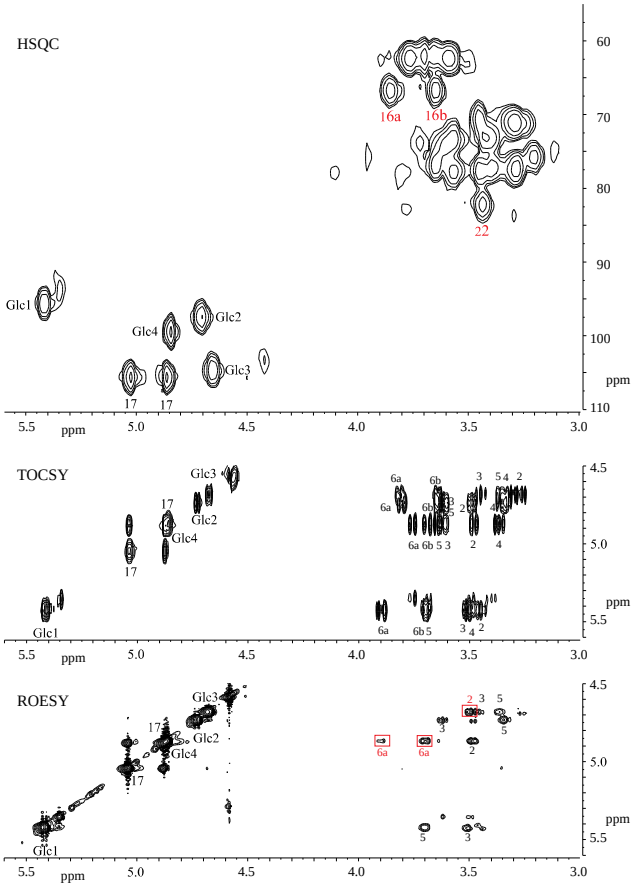

Figure S2. HSQC, TOCSY and ROESY spectra of the carbohydrate part of Stev-G2, recorded in D_2O at 310 K. In the HSQC spectrum, 22 means cross-peak H-2/C-2 of residue Glc2, etc. Assignments in red reflect the substituted positions of the residues. In the ROESY spectrum, the inter-residual cross-peaks confirming the Glc3(β1→2)Glc2 and Glc5(α1→4)Glc4(α1→6)Glc1 linkages are indicated with red boxes.